IEEE Access
Multidisciplinary ⋮ Rapid Review ⋮ Open Access Journal

Received 5 May 2024, accepted 22 May 2024, date of publication 27 May 2024, date of current version 3 June 2024.

Digital Object Identifier 10.1109/ACCESS.2024.3405572

METHODS

supDQN: Supervised Rewarding Strategy Driven Deep Q-Network for sEMG Signal Decontamination

ASHUTOSH JENA[1], NAVEEN GEHLOT[1], (Graduate Student Member, IEEE), RAJESH KUMAR[1], (Senior Member, IEEE), ANKIT VIJAYVARGIYA[2,3], (Senior Member, IEEE), AND MAHIPAL BUKYA[4], (Senior Member, IEEE)

[1]Department of Electrical Engineering, Malaviya National Institute of Technology Jaipur, Jaipur 302017, India
[2]Insight Science Foundation Ireland Research Centre for Data Analytics, School of Human and Health Performance, Dublin City University, Dublin 9, D09 V209 Ireland
[3]Department of Electrical Engineering, Swami Keshvanand Institute of Technology, Management and Gramothan, Jaipur 302017, India
[4]Department of Electrical and Electronics Engineering, Manipal Institute of Technology Bengaluru, Manipal Academy of Higher Education, Manipal, Udupi, Karnataka 576104, India

Corresponding author: Mahipal Bukya (mahipal.bukya@manipal.edu)

This work involved human subjects or animals in its research. Approval of all ethical and experimental procedures and protocols was granted by the Institute Ethics Committee (IEC) MNIT Jaipur.

ABSTRACT The presence of muscles throughout the active parts of the body, such as the upper and lower limbs, makes electromyography-based human-machine interaction prevalent. However, muscle signals are stochastic and noisy, with noises being both regular and irregular. Irregular noises due to movements or electrical switching require dynamic filtering. Conventionally, filters are stacked, which unnecessarily trims and delays the signal. This study introduces a decontamination technique involving a supervised rewarding strategy to drive a deep Q-network-based agent (supDQN). It applies one of three filters to decontaminate a 1 sec long surface electromyography signal, which is dynamically contaminated. A machine learning agent identifies whether the signal after filtering is clean or noisy, generating a reward accordingly. The identification accuracy is enhanced by using a local interpretable model-agnostic explanation. The deep Q-network is guided by this reward to select the filter optimally while decontaminating a signal. The proposed filtering strategy is tested on four noise levels (-5 dB, -1 dB, $+1$ dB, $+5$ dB). supDQN filters the signal desirably when the signal-to-noise ratio (SNR) is between -5 dB to +1 dB but filters less desirably at high SNR ($+5$ dB). A normalized root mean square (Ω) is formulated to depict the difference of the filtered signal from the ground truth. This is used to compare supDQN and conventional methods, including wavelet denoising with debauchies and symlet wavelet, high-order low-pass filter, notch filter, and high-pass filter. The proposed filtering strategy gives an average Ω value of 1.1974, which is lower than that of the conventional filters.

INDEX TERMS Deep reinforcement, EMG decontamination, motion artifact, powerline interference, white noise, biomedical measurement.

I. INTRODUCTION

Surface electromyography (sEMG) applications have increased rapidly in the past two decades and are still accelerating. According to data from the Web of Science, the number of studies on sEMG per year has gone from 32 in 2003 to 445 in 2022 [1]. In these studies, the most commonly observed applications of sEMG signal are rehabilitation, robotic prosthesis, medical diagnosis, gesture-controlled robotics, analysis, medical research, etc [2], [3], [4]. While all these studies consider using machine learning and artificial intelligence to achieve the task, the raw sEMG signal requires

The associate editor coordinating the review of this manuscript and approving it for publication was Hasan S. Mir.

a highly accurate and precise pre-processing methodology to remove noise. In sEMG signal, these noises are usually referred to as noise or contaminants in signal, which can be caused by motion artifact (MOA), physiological interference, powerline interference (PLI), white Gaussian noise (WGN), amplifier saturation, fatigue muscles, etc [5]. Removing such contaminants is necessary to avoid deviation from the actual outcome of these studies. Therefore, there is a need to identify and remove these contaminants from an sEMG signal.

Significant efforts have been made to decontaminate an sEMG signal. The most common decontamination techniques used in sEMG signal pre-processing are bandpass filtering (BPF) and notch filtering (NF). BPF is used to reduce the power level of samples having a frequency beyond the range of sEMG signals, while NF is used to do the same for a specific frequency, which reduces the PLI level in the signal [6], [7], [8]. However, these are static filters that act on the entire signal. Which can result in a reduction in power levels of the actual sEMG signal. The advanced form of filtering includes wavelet denoising [9], decompositional filtering techniques [10] and signal whitening [11]. Wavelet denoising is a premature technique that removes coefficients beyond a defined threshold. It is very useful in analysis. While the decompositional filtering techniques are very efficient, they are difficult to tune. The selection of the mother wavelet and degree of decomposition is a very hectic task. The more robust methods ICA and PCA are introduced in [12], [13], and [14]. These methods can reliably separate noises of different kinds however, ICA fails when the source of the signal is Gaussian in nature (as in sEMG and WGN) [15], additionally they are not adaptive and they are usually effective, only at a high power level of noise. As the noise level reduces, they fail to identify, making it difficult to separate noise from clean signal.

There are learning-based adaptive filtering methods employing variants of least mean square algorithms to tune the weights of a finite impulse response (FIR) or infinite impulse response filter (IIR) based filter [16], [17]. These filters are widely used in fetal ECG denoising using the mother's ECG signal as a reference signal [18]. While its applications are ubiquitous, the major drawback of these filters is the requirement of a reference signal at all times to determine the coefficients of filters. Generally, sEMG signal acquisition does not involve the acquisition of a reference signal. Moreover, depending on the algorithm, such filters also take substantial time to settle at a final coefficient for the FIR or IIR filter. Therefore, they are not popular among sEMG signal filtering. Recently, in [19], Iqbal demonstrated the use of an autoencoder in generating filtered signals out of contaminated seismic signals. A similar strategy is also followed in [20] to denoise ECG contaminated with EOG and EMG signals. However, both auto-encoder-based techniques are similar to adaptive filtering and employ a ground-truth signal during training. Usually, ground truth signal labeling requires a denoised signal with high fidelity. Due to the lack of standardization of sEMG signals, it is difficult to obtain ground truth. The other important issue is converting the 1-D signal to a 2-D image in the pre-processing stage, using short-time discrete cosine transformation. This transformation from 1-D to 2-D can significantly impact deployable models. Deployable models have time and memory constraints, and processing in 2-D may affect adverse. A brief comparison of the same is highlighted in [21]. Due to the dynamic and unpredictable nature of sEMG signals, most of these approaches fail to address justified filtering. Therefore, in most of the application-oriented articles, it can be observed that the popular filtering methods among them remain to be LPF, BPF, HPF, and wavelet denoising techniques due to their simplicity in usage and efficiency performance, without affecting the analysis greatly.

However, reinforcement learning (RL) methods have proven very suitable under such dynamic environments. Apart from its wide applications in robotics and games [22], [23], it has also been used in signal processing. In the past, Sahba and Tizhoosh have demonstrated the use of multiple filters optimally selected by an RL agent to filter an image in [24]. The agent in their study would select the weight values of different filters to obtain an image with a higher SNR. Other RL applications in image denoising have been demonstrated in [25] and [26]. In [27], Liang et al. have used an asynchronous advantage actor-critic (A3C) agent to dynamically alter the denoiser to denoise complex and diverse seismic signals. In [28], hand gesture recognition using sEMG signals is achieved with deep Q-learning and double deep Q-learning. In all these studies, implementing RL to those problems requires formulating the problem as a Markov decision process (MDP). In [29], Tosin and Balbinot formulated noise removal as an MDP and dynamically filtered four different types of noise introduced at different intervals of a signal. They considered an actor-critic agent with a fuzzy logic-based rewarding strategy to achieve optimal noise filtering. The fuzzy logic-based rewarding strategy requires an inference table, which can only be determined by an expert. However, in [29], the authors deduced a heatmap-based fuzzy inference table before the learning process. This heatmap table guides the output of the fuzzy system, which is then used to generate a reward. This becomes tedious when a change in noise level is introduced.

This forms the motivation of this article to develop an automated signal decontamination technique with the help of a supervised rewarding strategy in reinforcement learning to select a filter optimally in a dynamically contaminated sEMG signal within an allowable time constraint. To address the issues above, a supervised rewarding strategy is proposed, which aims to simplify and diversify the reward generation process while improving efficiency at each step of reward generation. At the same time, a reinforcement learning agent capable of solving this problem efficiently is obtained, tested,

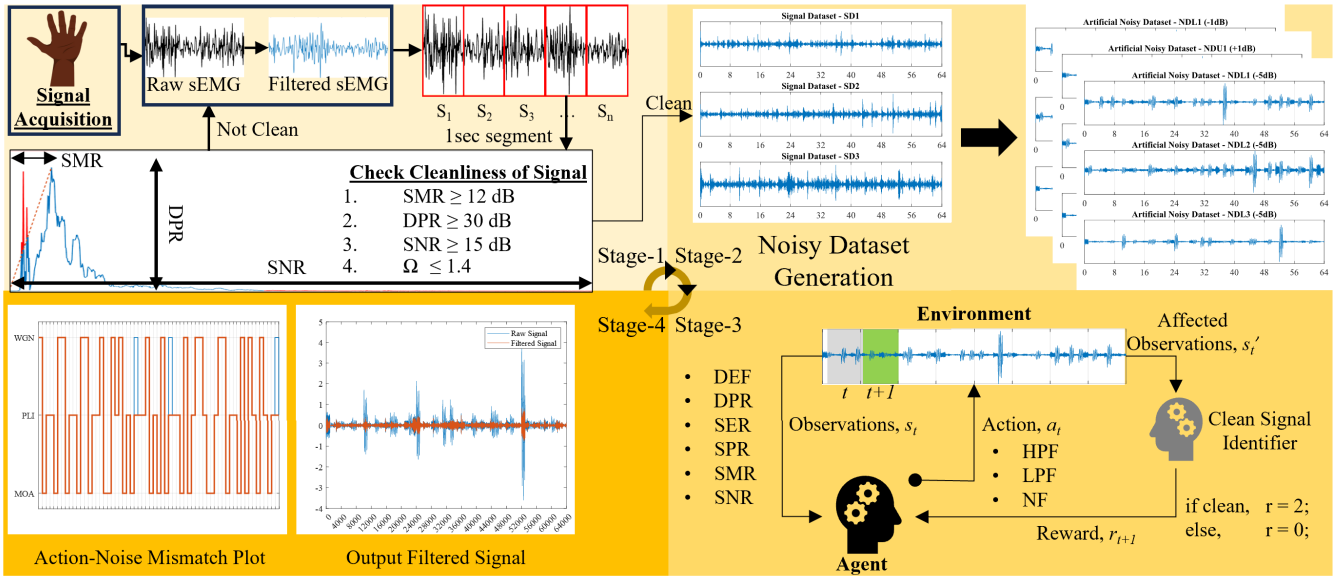

FIGURE 1. Flow of study: Stages 1 and 2 deal with artificial contamination of a clean sEMG signal. They have been discussed in Section II under the subtopics of signal cleaning and artificial contamination, respectively. Stage 3 deals with the methodology of proposed filtering and it has been discussed in Section III. Stage 4 is the results and comparative analysis which is discussed in Section IV.

and evaluated. Desirably, such an agent should display the following characteristics:

- It should respond to different noises dynamically.
- Its computational complexity must be within a limited range.
- It must be independent of the ground-truth signal.

The main applications of the proposed method may include denoising signals exposed to dynamic changes in noises, denoising signals with non-stationary characteristics, and recurring signals with irregular noises, such as biopotential signals like EEG and EMG. Due to the lack of standardization and availability of ground truth signals during the acquisition, these signals are better suited for application with the proposed method.

The work done in this study is as follows:

- A deep Q-network-based learning agent that learns to identify and decontaminate an sEMG signal dumped with three different noises at different intervals.
- A new and efficient reward generation strategy involving machine learning agents (MLA) is proposed to decontaminate sEMG signals. To improve the efficiency of the MLA, a local interpretable model-agnostic explanation (LIME) tool is used to interpret and finally select the optimal set of features.

The upcoming sections are organized as follows: The problem is introduced in Section I. Section II and III present the foundation of the dataset and the proposed filtering method, respectively. The result with analysis is discussed in Section IV. Section II - IV are the four stages described in FIGURE 1 indicating the flow of the study. Finally, the study is concluded in Section V.

II. DATASET

This section presents the artificial generation method of noisy sEMG signals for the study. Mathematically, the artificial contamination can be represented in equation (1). This equation represents a general idea of the addition of noise (n(t)) on top of a clean signal (x(t)) at a level decided by the value of A to obtain a noisy sEMG signal (y(t)).

$$y(t) = x(t) + A \times n(t) \tag{1}$$

For the study, three clean signals are obtained following the procedure described in Section II-A. Three different types of noise (MOA, PLI, and WGN) are considered, which is elaborated in subsection II-B. The other noises are physiological (electrocardiogram (ECG)) and instrumental noise, which are not considered in the study due to a lack of standardization in integrating ECG with sEMG to produce noisy sEMG and a lack of a model to represent instrumental noise. Subsection II-B also explains the procedure of contamination. The reliability of the filtering agent is checked at the different SNRs: −5 dB, −1 dB, +1 dB, and +5 dB. The outcomes of this section are nine noisy sEMG datasets at four different noise levels.

A. SIGNAL CLEANING

sEMG signal is acquired using a BIOPAC MP150 device [30]. The signal is acquired while the subject holds a book for 2 minutes. The acquisition frequency is 2 kHz, and only one channel is used. For a proper analysis, the procedure mentioned above is repeated ten times while holding the book in different ways, as shown in FIGURE 2. Since the study revolves around the identification and removal of noise,

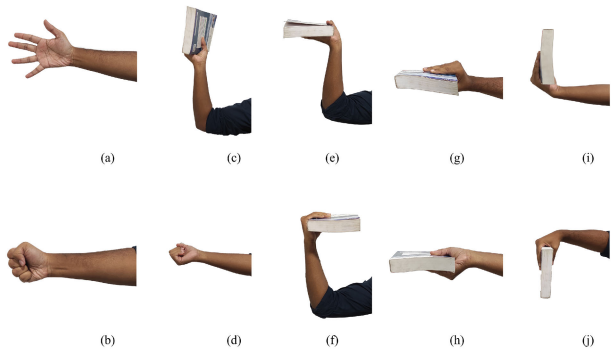

FIGURE 2. The ten hand activities performed to obtain sEMG signals.

the cleanest possible form of sEMG signal is acquired by setting up the options for low-pass filtering. Any value of the frequency component above the range occupied by the sEMG signal [31] is filtered using the 500 Hz LP mode of filtered signal acquisition. The acquired signal, however, is not free of low-frequency MOA and PLI. These noises are filtered using digital filters, and a signal purity check is performed using the method described in [32]. The purity of the signal is checked over a window of 1 sec following the constraints given in TABLE 1. If the SMR, SNR, DEF, and DPR values are inside the acceptable range, it is marked 'good'. It is intuitively deduced that if the percentage of total good marked segments over the entire signal is above 90%, the signal can be assumed to be suitable. However, if a signal is found impure, it is discarded. The pre-processed signal obtained at the end of this stage is referred to as a clean signal in further stages. For

TABLE 1. Constraints to check purity of signal [32].

Features	Acceptable Range
Signal to motion artifact ratio (SMR)	SMR $\geq$ 12 dB
Signal to noise ratio (SNR)	SNR $\geq$ 15 dB
Power density (DPR)	DPR $\geq$ 30 dB
Deformation ratio (DEF)	DEF $\leq$ 1.4

a generalized analysis, two conditions need to be fulfilled by the clean signal datasets:

- The signals to be considered should be different from each other based on activity.
- The signals must fulfill the cleanliness criteria as shown in TABLE 1.

Initially, ten raw sEMG datasets are obtained with a length of 96 sec. After filtering and signal purity checks, it is observed that only one sEMG dataset (sEMG-10) is suitable in the length of 96 sec (refer, TABLE 2). Since, considering the 96 sec long signal violates the conditions for generalized analysis, two more signals close to 90% clean are explored (sEMG-6 and sEMG-9). Dividing these three signals (sEMG-6, sEMG-9, and sEMG-10) further into 32 sec long signals, it is observed that the conditions are fulfilled (refer to TABLE 3). These three clean signals of length 32 sec are selected for the study.

TABLE 2. Signal cleanliness checked over 96 sec long signals.

Signals	sEMG-1	sEMG-2	sEMG-3	sEMG-4	sEMG-5
Cleanness (%)	79.17	57.29	15.10	69.79	11.98
Signals	sEMG-6	sEMG-7	sEMG-8	sEMG-9	sEMG-10
Cleanness (%)	89.58	30.73	59.89	84.89	93.75

TABLE 3. Signal cleanliness checked over 32 sec intervals.

Signals	Percent cleanliness (in %)			Nomenclature
	0-32 sec	32-64 sec	64-96 sec	
sEMG-6	87.5000	85.9375	**95.3125**	SD1
sEMG-9	81.2500	**90.6250**	82.8125	SD2
sEMG-10	**95.3125**	93.7500	92.1875	SD3

B. ARTIFICIAL CONTAMINATION

The three clean sEMG signals are used to obtain nine noisy sEMG signals. The three noises used for doping with a clean signal include MOA, PLI, and WGN. These noises are added randomly to the signal in windows of 500 msec. Three random sequences are prepared, as shown in FIGURE 3. After these three sequences, noises are added to the three clean datasets, forming nine noisy sEMG datasets. The information regarding the dataset of noise used during noise addition is described in brief as follows:

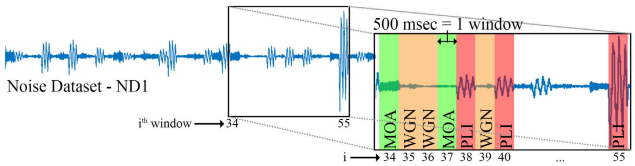

FIGURE 3. Illustration of noise added in random sequence.

1) MOTION ARTIFACT

MOA is a low-frequency and high-power level artifact with a typical frequency range of 0.5 to 20 Hz. It is a result of skin-electrode interface movement. It cannot be generated. Therefore, it is collected using the BIOPAC MP150 DAQ setup. However, while collecting the signal for MOA, a series of 50-60 taps are done in the proximity of the electrode-attached muscle in one minute [29]. To retain only the signal containing MOA, the obtained signal is filtered beyond 35 Hz using a low pass filter with a cutoff frequency of 35 Hz. The resulting signal is assumed to be a purely MOA noise.

2) POWERLINE INTERFERENCE

PLI is electromagnetic interference occurring due to the electrical devices in proximity to the acquisition setup. It affects the frequency domain, specifically at the powerline frequency. In the study, PLI is a sine function as represented in equation (2)

$$n_{PLI}(t) = \sin(2\pi \times 50t) + \frac{1}{3}\sin(2\pi \times 150t) \qquad (2)$$

3) WHITE GAUSSIAN NOISE

WGN is a Gaussian noise distributed throughout the frequency domain with a low power level. Since it is distributed in the entire frequency range, its filtering is the most difficult. However, [5], [33] suggests that removing the signal after 500 Hz should effectively improve the SNR of the signal. Data for WGN is obtained using the *wgn* function in MATLAB with a random power level between -8 and -4 dB. In equation (3a), r is a random variable obtained from the set of real numbers uniformly distributed over the range of -8 and -4 dB.

$$r \in \mathbb{N} \cap [-8, -4] \tag{3a}$$

$$\mathrm{n_{WGN}}(t) = \mathrm{wgn}(r) \tag{3b}$$

The final noisy datasets (NDs) are prepared by adding $\mathrm{n_{moa}}(t)$, $\mathrm{n_{pli}}(t)$ and $\mathrm{n_{wgn}}(t)$ to the main signal dataset (SD) in a pre-defined random sequence. This can be mathematically expressed as follows:

$$y_{ijk}(t) = x_{j_i}(t) + \alpha(p_{k_i}\mathrm{n_{moa}}(t) + q_{k_i}\mathrm{n_{pli}}(t) + r_{k_i}\mathrm{n_{wgn}}(t))\ \forall i \tag{4}$$

Here, $p_{k_i}, q_{k_i}, r_{k_i} \in \{0, 1\}$ and $p_{k_i} + q_{k_i} + r_{k_i} = 1\ \forall\, i \in \mathbb{Z}^+ \cap [1, T]$. $x_{j_i}(t)$ represents the 1000 samples long i^{th} segment of the j^{th} clean signal. T represents the total timesteps in an episode. $y_{jk}(t)$ corresponds to the i^{th} segment of final noisy signal obtained out of j^{th} clean signal doped with noise following k^{th} noise sequence. Here, $j, k \in \{1, 2, 3\}$. 'α' indicates the level of noise, and it is given by the following equation,

$$\alpha = \frac{P_c}{P_n \times (10^{0.1\ P_{\text{req}}} - 1)} \tag{5}$$

Here, P_c, P_n, P_{req} represents the power level of the clean signal, noise signal, and required SNR in dB, respectively.

III. METHODOLOGY

The filtering problem considered in this study is viewed as a reinforcement learning problem. A DQN agent-based reinforcement learning environment is set up to achieve dynamic filtering of an sEMG signal. Where the goal of the agent is to minimize the noise appearing in the signal by taking suitable filtering action. FIGURE 4 depicts the flow of the algorithm. The three key components of this algorithm are environment setup, rewarding strategy, and agent learning. At any timestep 't', six features are extracted from a segment of signal seg_t. These features constitute the observations at that timestep. Viewing the observation, the agent takes a filtering action on the current segment (seg_t) following an $\epsilon-$greedy policy. The features corresponding to this filtered segment are input to a pre-trained machine learning agent (MLA) to generate reward based on clean or noisy. The reward is used to update a deep network for Q-value estimation, which is called a critic network. Finally, the timestep is incremented in which the next segment of signal (seg_{t+1}) becomes the next observation. The subsequent sections elaborate all these procedures.

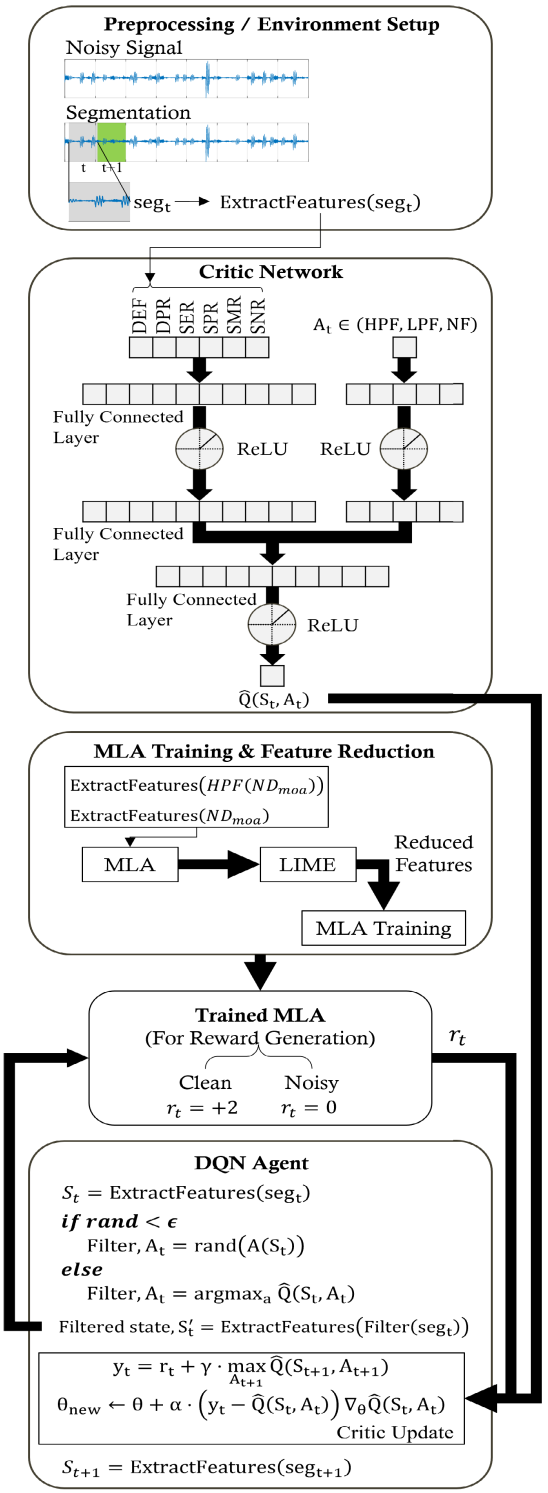

FIGURE 4. Overall flowchart of proposed methodology.

A. sEMG ENVIRONMENT SETUP

The sEMG signal is treated as the environment in which a timestep increment is observed over a window of 500 msec of the signal. At timestep, t = 1, the first 500 msec of the signal becomes the current observational segment, and the subsequent 500 msec becomes the next observational

segment for t = 2. Therefore, a maximum of 64 timesteps are possible in a particular episode. At the end of Section II-B, nine noisy sEMG datasets (NDs) are formed. One of the nine is used for training (ND1), and the rest are for testing and evaluation (ND2-ND9). After the training, four supDQN filtering agents are formed, each for a specified SNR level.

1) OBSERVATIONS

The physical significance of observation in any environment is the physical values that may represent the situation of the environment at that timestep. In this case, at any timestep, the environment can be represented by deformation ratio (DEF), peak density (DPR), signal-to-motion artifact ratio (SMR), signal-to-noise ratio (SNR), signal-to-powerline ratio (SPR) and signal-to-electrocardiogram ratio (SER). There can be more observations from the environment at any particular timestep. However, their values may be insignificant from the perspective of the goal. Procedures to compute these physical parameters are referred from [29] and [32].

2) ACTIONS

Actions are the tasks that an agent performs on its environment at any particular time step. In this case, filtering the raw signal is considered the action. The different actions that the agent is equipped with are high pass filtering (HPF) against MOA, low pass filtering (LPF) against WGN, and specific frequency notch filtering (NF) against PLI. The filters are digital elliptic filters with an 80 dB attenuation. Elliptic filters are chosen for their better steady-state response even at a reduced order of the system. At any timestep, the agent observes the environment it is currently in and then takes action following a policy. The task of the supDQN agent is to obtain a policy that yields the highest Q-value over an episode. The supDQN agent and the Q-value are defined in Section III-B.

3) REWARDING STRATEGY

Reward is the performance measure of an action. To obtain an optimal policy, the reward must be a positive incentive for good and a negative incentive for wrong action. It can be represented as a function of state (s) and action (a). However, due to the stochastic nature of an sEMG signal and its features (i.e., observations at every timestep), it is necessary to use a trained MLA to distinguish good action from bad. Therefore, during the study, the reward for an action is determined by an MLA, trained with the training dataset to identify clean and noisy signals.

In this context, the training dataset is obtained by adding a specific noise to the clean signal (SD1). The cleaned version of this signal is obtained by filtering it with a noise-specific filter. In this case, the noise-specific filter is HPF for MOA, NF for PLI, and LPF for WGN. All the other combinations of actions and noise are labeled as noisy. Therefore, the dataset consists of two signals labeled as noisy and clean for a single action. This dataset is pre-processed,

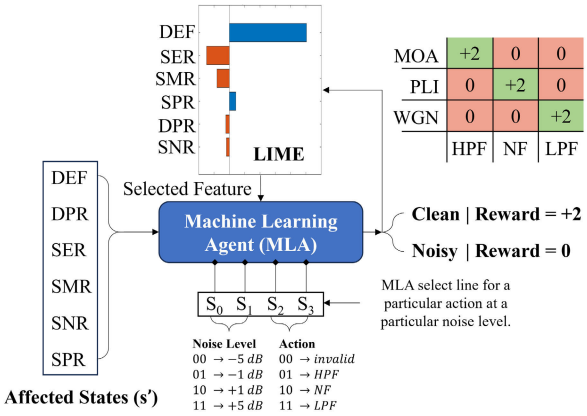

FIGURE 5. Rewarding strategy.

in which the six features (DPR, DEF, SER, SMR, SNR, SPR) are extracted from the signals. Using this feature-based dataset, six of the widely used MLAs, including support vector machine (SVM) [34], linear discriminant analysis (LDA) [35], artificial neural network (NN) [36], decision tree, logistic regression, and k-nearest neighbors are trained to perform binary classification.

However, only one MLA is selected based on maximum accuracy. The LIME analysis is performed on the selected MLA to study the relevance of features in enhancing MLA's accuracy. The outputs from LIME (refer to FIGURE 6) suggest that in some cases, a few out of the six states/features can be used for noise identification and improve the accuracy of that model [37], [38], [39]. The length of the bar in the FIGURE 6 represents that feature's ability to improve the identification of either noise (red bar) or clean (blue bar). Hence, the features not contributing to a higher accuracy are eliminated from the bottom of the list in each case, and the same classifier is trained again with the reduced feature set. Since every filtering action affects the signal environment differently, it is necessary to find a fitting MLA for each action in every environment to generate the correct reward. Therefore, three MLAs are selected for three actions, and each MLA is tuned optimally to correctly generate a reward signal with high accuracy.

The study is extended with a reliability analysis of other noise levels. Four noise levels are considered (−5 dB, −1 dB, +1 dB, and +5 dB) to achieve this. Usually, the SNR value varies with a very low standard deviation unless a major change appears during acquisition. Therefore, for simplification in analysis, it is assumed that SNR remains fixed during acquisition. Based on this assumption, the denoising agent is proposed to be trained with a noisy dataset at a fixed SNR. Therefore, when the SNR changes to a new value, re-training of these MLAs is required to improve the accuracy of the rewarding function at the new SNR. Since, in this study, reliability analysis is done on four SNRs, and each SNR requires three trained MLAs, 12 trained MLAs are listed in TABLE 4 with their corresponding input features. Therefore, TABLE 4 can be interpreted as follows: if the

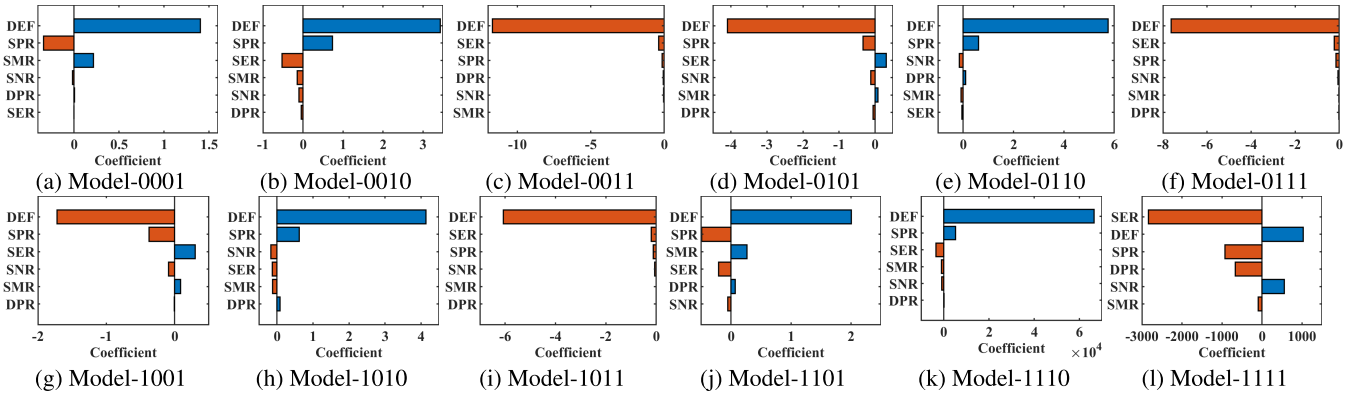

FIGURE 6. Outputs of LIME for various models.

reliability of denoiser is being evaluated for SNR= −5 dB, and the agent takes an Action = HPF, a trained neural network-based MLA is selected to identify and generate reward.

The reward for the reinforcement learning (RL) agent is dependent on the current action, level of noise, and the filtered states. For instance, if the current action is LPF at noise level SNR = −5 dB, the MLA will consider only four features (i.e., DEF, DPR, SER, SPR) out of the six filtered states as input and perform classification and generate a reward based on the predicted label. A reward of +2 is awarded when the predicted label is clean else a reward of 0 is given to the MLA. The complete rewarding strategy is pictorially represented in FIGURE 5. Here, the MLA select line is a four-bit binary select line that uses only 12 states to merely select an MLA for a particular action and a noise level.

TABLE 4. List of MLAs employed for reward generation due to each action at various noise levels.

S_1S_2 S_3S_4	Noise Level (in dB)	Action	Extracted Features	MLA	Model Accuracy (in %)
0001	-5	HPF	All	NN	89.1
0010	-5	NF	DEF, SER, SMR, SPR	SVM	90.2
0011	-5	LPF	DEF, DPR, SER, SPR	SVM	76.4
0101	-1	HPF	All	NN	96.6
0110	-1	NF	All	NN	98.9
0111	-1	LPF	All	SVM	94.8
1001	+1	HPF	All	NN	97.7
1010	+1	NF	All	SVM	98.9
1011	+1	LPF	All	SVM	96.0
1101	+5	HPF	All	SVM	73.0
1110	+5	NF	All	SVM	72.2
1111	+5	LPF	All	LDA	64.9

B. SUPERVISED REWARD BASED DEEP Q-NETWORK (supDQN) AGENT

Deep Q-learning (DQN) is an extension of the Q-learning algorithm. It combines deep learning with the existing knowledge of Q-table update [23]. When the state space is continuous, it becomes difficult to contend all the states in a Q-table. In such cases, a universal function approximator like a deep neural network can be considered to estimate the Q-values. This function approximator is generally parameterized in θ, and it learns to approximate much better by minimizing a loss as given in equation (6)

$$\mathrm{L_i}(\theta_i) = \mathbb{E}_{s,a,r,s'\sim p(.)}((y_i - \mathrm{Q}(s,a;\theta_i))^2) \tag{6a}$$

$$y_i = r + \gamma \max_{a'} \mathrm{Q}(s',a';\theta_{i-1}) \tag{6b}$$

Where $\mathrm{L_i}(\theta_i)$ is the loss function for the Q-value approximator network. It is equal to the expected temporal difference (TD) of the TD target (from the previous iteration) and estimated Q-value in the present iteration (i). y_i represents the Q-value estimation parameterized over θ_{i-1} (θ at previous iteration) and γ is the discount factor. $\mathrm{Q}(s,a;\theta)$ represents the Q-value function of state s and action a, parameterized in θ.

In this study, while the states for the training environment (ND1) are fixed and discrete in 64 timesteps, a Q-learning algorithm is suitable for learning the optimal policy to reduce noise. However, as the environment changes during testing or implementation, the Q-table fails to adjust the new states in the Q-table because the states are continuous in this case, resulting in the agent's failure. The Q-value is estimated using a deep neural network for continuous state/observation (s) and discrete action (a).

$$\mathrm{Q}^*(s,a;\theta) = \mathbb{E}[r + \gamma \max_{a'} \mathrm{Q}^*(s',a';\theta)] \tag{7}$$

$\mathrm{Q}^*(s,a;\theta)$ is the quality of taking action a, starting from state/observation s and following the optimal policy path thereafter parameterized over θ (also known as optimal Q-value function). Mathematically this is equivalent to the expected immediate return (r) plus the discounted future optimal return ($\gamma \max_{a'} \mathrm{Q}^*(s',a';\theta)$). Here, s' represents states/observations at the next timestep, which differs from affected states explained in Section III-A3. Since the DQN agent is driven by a supervised learning-based rewarding strategy, it is named supDQN. Once the supDQN is trained, the Q-value estimator network stops updating its parameter θ. When this trained model is simulated, the trained estimator network (shown as critic network in FIGURE 4) directly estimates the Q-value from the input states and actions and

follows the path of the learned policy. As it tries to maximize the return, the signal is more filtered.

C. AGENT PERFORMANCE EVALUATION

In Section II-B, noises are introduced in specified segments. The sequence of actions being taken at each segment is noted and checked to see if the specific action helps reduce the noise. In Section III-A2, intuitively, it is found that action HPF, LPF, and NF are best equipped against MOA, WGN, and PLI, respectively. Therefore, during the study, a desired set of actions was already known to be against the type of noise added at every segment. While evaluating the trained supDQN agent, whether the agent acts according to the desired set of actions is checked. The accuracy of the agent is calculated using the following equation

$$\text{Acc} = \frac{\text{Total timesteps} - \text{number of missed actions}}{\text{Total timesteps}} \times 100 \tag{8}$$

Here, missed actions are the actions that deviate from the desired actions at any timestep. The missed actions and the agent's precision can be judged by using confusion matrices. The confusion matrix shows how the agent takes action against a particular type of noise in an environment. Noise 1, 2, and 3 correspond to MOA, PLI, and WGN, respectively, whereas actions 1, 2, and 3 correspond to HPF, NF, and LPF, respectively. Similarly, an action plot is plotted against the timesteps in the x-axis. In the action plot, if the orange line overlaps completely with the blue line, the action taken is the same as the desired action. The filtered signal plot compares the noisy signal after being filtered by the supDQN agent (orange) against the original noisy signal (blue).

This filtering technique is compared against conventionally used filtering methods based on an error parameter (Ω) which is calculated as follows

$$\Omega = \frac{\sqrt{\frac{1}{N}\sum_{i=1}^{N}(y_i - x_i)^2}}{\sqrt{\frac{1}{N}\sum_{i=1}^{N}(n_i - x_i)^2}} \tag{9}$$

where y_i, x_i, and n_i represent the i^{th} sample of the filtered, clean, and noisy signals, respectively. A lower value of Ω indicates a more clean signal. The conventional filtering methods are compared against the proposed supDQN-filtering agent based on this parameter later in TABLE 6.

IV. RESULT AND ANALYSIS

In this section, the output from the resulting supDQN filter is analyzed and compared with that of the conventional filters which include wavelet denoisers (with debauchies (dB4) and symlet (sym4) wavelet), low order high pass, low pass, notch pass filter, and threshold-based denoising of individual intrinsic mode functions in the time-domain using empirical mode decomposition [40]. To execute this, the entire study is carried out in a 12th generation Intel core i7 processor with an installed RAM of 16.0 GB capacity. MATLAB R2023a platform is used to execute all the programs and analyze results. Four cases for four different noise levels are prepared.

A. CASE I: NOISE LEVEL −5 DB

In all the cases, the training environment is the ND1 dataset, and the rest of the environments (ND2 to ND9) are used as test environments to validate the agent. In this case, the noise is added such that the SNR corresponding to each segment is −5 dB. The three MLA for reward generation are referred from TABLE 4. The agent-DQ1 is trained for 2000 episodes, each with a maximum of 64 timesteps. The learning rate of the deep neural network is 0.001, and an Adam optimizer with a gradient decay of 0.9 and l^2norm gradient thresholding is used to optimize the weights of the neural network. The exploration rate varies from 0.6 to 0.05, with a 0.003 decay at every timestep. The simulation on the testing dataset is observed, and its performance analysis recorded while testing ND2 and ND3 is shown in FIGURE 7.

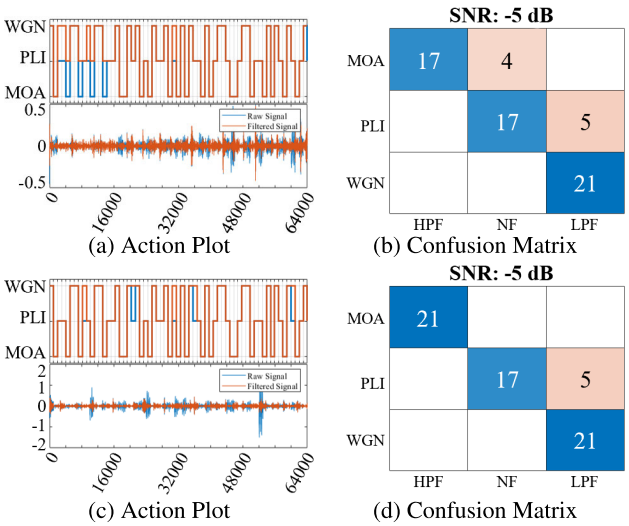

FIGURE 7. Performance of supDQN agent at a noise level of −5 dB.

FIGURE 7a-7b are the simulation results with the supDQN agent acting on dataset ND2 at a noise level of −5 dB. Whereas FIGURE 7c-7d are the simulation results with supDQN agent acting on dataset ND3 at a noise level of −5 dB. FIGURE 7 suggests that at this noise level, the supDQN agent acts against the desired action 14 times while correctly identifying and filtering contaminant at 114 different timesteps. For the rest of the environments, only the accuracy and error ratio parameter Ω associated with the testing environment is mentioned in TABLE 5 and TABLE 6, respectively. The optimizer settings for the estimator network and the exploration decay rate are the same for the rest of the cases.

B. CASE II: NOISE LEVEL −1 DB

The agent-DQ2 is trained and tested on the sEMG environment, including a −1 dB noise level at different

segments. The simulation results are shown in FIGURE 8. It suggests that the supDQN agent fails to follow the desired action in 5 cases and correctly identifies and decontaminates the signal in 123 different timesteps.

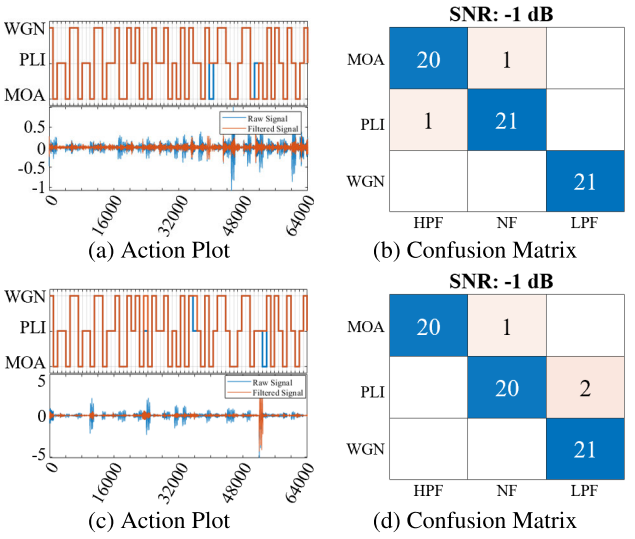

FIGURE 8. Performance of supDQN agent at a noise level of −1 dB.

C. CASE III: NOISE LEVEL +1 DB

The agent-DQ3 is trained and tested on an sEMG environment with a +1 dB noise level at different segments. The simulation results are shown in FIGURE 9. It suggests that the supDQN agent fails four times and correctly identifies and decontaminates the signal 124 times.

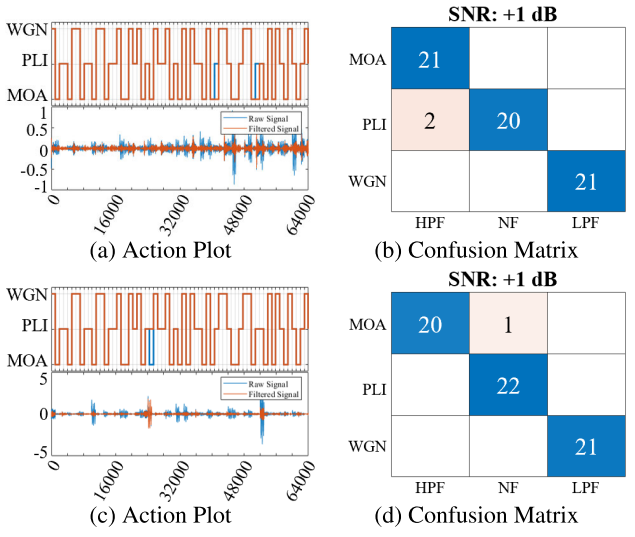

FIGURE 9. Performance of supDQN agent at a noise level of +1 dB.

D. CASE IV: NOISE LEVEL +5 DB

The agent-DQ4 is trained and tested on an sEMG environment with a +5 dB noise level at different segments. The simulation results are illustrated in FIGURE 10. It suggests that the supDQN agent fails in 88 timesteps and succeeds in 40 timesteps. This happens due to the low impact of noise at this SNR level. At this level of SNR, it becomes difficult for machine learning agents to distinguish between noisy and clean signals based on the six features (DEF, DPR, SER, SMR, SNR, and SPR). For better distinction, there is a need to exploit additional features that can prove helpful for noise identification at this noise level.

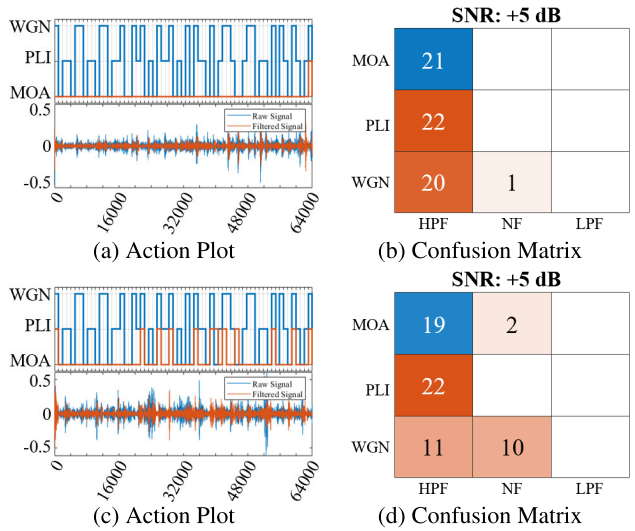

FIGURE 10. Performance of supDQN agent at a noise level of +5 dB.

TABLE 5 presents the accuracy of supDQN agents in following the desired policy at different noise levels for all the testing datasets.

TABLE 5. Accuracy (in %) of supDQN at following the desired actions in different noisy sEMG environments and at different noise levels.

	ND2	ND3	ND4	ND5	ND6	ND7	ND8	ND9
-5 dB	85.94	92.19	92.19	82.81	93.75	93.75	82.81	92.19
-1 dB	95.31	96.68	96.87	96.87	96.87	96.87	93.75	95.31
+1 dB	98.44	95.31	96.87	98.43	93.75	98.44	98.44	96.87
+5 dB	32.81	29.69	29.69	32.81	31.25	31.25	31.25	29.69

TABLE 6 shows the performance of supDQN compared to the performance of other filters. Each filter's performance is evaluated using equation (9) at different noise levels for each test environment. The resulting values are then compared. Due to the consistency in maintaining the minimum Ω of 1.1974, which is expressed by the mean Ω in TABLE 6, it can safely be said that the supDQN decontaminates a mixed noise signal more effectively compared to the other filtering techniques. In 23 out of 32 cases, it performs better than the rest, and in 4 cases, it performs better than most filtering methods except HPF. In FIGURE 10, it can be observed that when the agent is unable to identify noises correctly, it takes the HPF action more likely compared to the other. It is an adaptable learning agent that quickly adjusts to new environments after a little training since the learning process is dynamic.

TABLE 6. Performance comparison table between the proposed method and conventional method.

SNR (in dB)	DS	WD (db4)	WD (sym4)	NF	LPF	HPF	EMD	supDQN
-5	**ND2**	2.5925	2.5923	2.5896	2.5715	1.7632	1.0431	1.0240
	ND3	0.8647	0.8646	0.8637	0.8525	0.6875	2.2146	0.5120
	ND4	0.9995	0.9993	0.9962	1.2414	1.3021	1.1040	0.8387
	ND5	1.6508	1.6506	1.6483	1.6345	1.1602	1.0271	0.7426
	ND6	1.2050	1.2049	1.2034	1.1882	0.9835	1.3247	0.6945
	ND7	0.9996	0.9995	0.9984	1.1959	1.1369	1.3051	0.7590
	ND8	1.4331	1.4330	1.4315	1.4171	0.9654	1.1161	0.6770
	ND9	0.9659	0.9659	0.9648	0.9489	0.7590	1.1821	0.5627
-1	**ND2**	0.7798	0.7797	0.7789	0.7735	0.5304	1.1656	0.3954
	ND3	0.2601	0.2601	0.2598	0.2564	0.2068	1.1353	0.7543
	ND4	0.9998	0.9997	0.9950	1.0016	0.4687	1.4946	0.4334
	ND5	0.4965	0.4965	0.4958	0.4916	0.3490	1.1015	0.8684
	ND6	0.3624	0.3624	0.3620	0.3574	0.2958	2.1697	0.3209
	ND7	0.9998	0.9998	0.9971	1.0002	0.4168	1.0760	0.4642
	ND8	0.4311	0.4310	0.4306	0.4263	0.2904	1.3037	0.7407
	ND9	0.2905	0.2905	0.2902	0.2854	0.2283	1.2647	0.8037
1	**ND2**	0.9817	0.9816	0.9806	0.9738	0.6677	1.1238	0.4523
	ND3	0.3274	0.3274	0.3270	0.3228	0.2604	1.1801	0.2877
	ND4	0.9997	0.9996	0.9950	1.0203	0.5669	1.2975	0.3772
	ND5	0.6251	0.6250	0.6242	0.6189	0.4393	1.0845	0.3377
	ND6	0.4563	0.4563	0.4557	0.4499	0.3724	1.8291	0.3210
	ND7	0.9998	0.9997	0.9968	1.0064	0.5148	1.0603	0.3652
	ND8	0.5427	0.5427	0.5421	0.5366	0.3656	1.3706	0.3215
	ND9	0.3658	0.3657	0.3653	0.3593	0.2874	1.1233	0.2959
5	**ND2**	8.1983	8.1976	8.1891	8.1319	5.5758	1.3072	5.0203
	ND3	2.7344	2.7343	2.7311	2.6957	2.1742	1.1742	1.9753
	ND4	0.9988	0.9984	1.0071	2.6387	4.0672	1.2200	3.8499
	ND5	5.2202	5.2198	5.2125	5.1687	3.6689	1.2841	3.2906
	ND6	3.8105	3.8103	3.8055	3.7575	3.1102	1.0671	2.8730
	ND7	0.9992	0.9989	1.0048	2.3431	3.5731	1.2209	3.2845
	ND8	4.5320	4.5317	4.5269	4.4814	3.0528	1.1869	2.6743
	ND9	3.0545	3.0543	3.0509	3.0007	2.4001	1.0440	1.9990
Mean Ω		**1.5680**	**1.5679**	**1.5662**	**1.6609**	**1.3325**	**1.2671**	**1.1974**

Abbreviations: DS: Dataset; WD: Wavelet denoisers; EMD: Empirical mode decomposition

E. COMPUTATIONAL COMPLEXITY

The computational complexity of any algorithm is the number of additions and multiplications involved in producing results. Time consumption analysis is an extension of this analysis, which provides an estimated time that might be consumed by different hardware to produce the result. A computational complexity analysis is provided for the proposed architecture for a generalized comparison. The proposed architecture involves the following
processes:

- A frequency domain transformation: $S\log(S)$
- Calculation of six features in the frequency domain: $6 \times \mathrm{O}(S/2)$
- Q - function approximation through neural network structure given in FIGURE 4: $\mathrm{O}(10D + 10(\text{bias}) + 10(\text{ReLU}) + 10 \times 10 + 10(\text{bias}) + 10(\text{ReLU}) + 5A + 5(\text{bias}) + 5(\text{ReLU}) + 5 \times 5 + 5(\text{bias}) + 5(\text{ReLU}))$
- Filtering using a single FIR filter, which involves convolution operation: $\mathrm{O}(N + S - 1)^2$
- Reward generation through an MLA: $\max(\mathrm{O}(1 \times D), \mathrm{O}(1 \times D^2), \mathrm{O}(87))$

Here, D represents a number of features in an observation, N represents the order of the employed filter, S represents a number of samples, and $A = 1$ represents a number of action inputs. The bias, ReLU, inside the parenthesis indicates the mathematical operation. TABLE 7 provides a comparative analysis of the computational complexity of stacked filters and the proposed method. Because filters must be stacked to achieve similar Ω values using the conventional method, this table highlights the necessity of employing a single filter rather than stacking filters to lower computations and achieve filtering in reduced time.

TABLE 7. Computational complexity comparison table.

Methods	Computaional Complexity
NF+LPF+HPF	$3 \times (N + S - 1)^2$
supDQN	$S\log(S) + 6S/2 + 492 + (N + S - 1)^2$

V. CONCLUSION

This study presented a dynamic noise reduction technique that showed supremacy over conventional filtering techniques. supDQN is an environment-interacting agent, and its ability to filter segment by segment enables it to react to noise dynamically. It allows the filtering agent to filter noises dynamically. To achieve this, a supervised MLA was used to generate a reward and properly direct the supDQN agent to filter optimally in an unknown sEMG signal environment. At a higher noise level in the signal (i.e., when SNR is -5 dB, -1 dB, or $+1$ dB), the MLA accurately identified clean from noisy signal, which ensured a better degree of contamination removal. However, when the noise level in the signal is low (i.e., when SNR is $+5$ dB or more), the noisy signal is similar to the clean signal, which causes difficulty for the MLA in distinguishing noisy from the clean signal. Therefore, the agent fails to follow the desired filtering actions at every timestep. However, it minimized noise better than conventional techniques (refer TABLE 6). The specific advantages that this technique provides over traditional methods are listed as follows:

- Environment interactive filter: It employs a feedback mechanism to dynamically feed the agent with the current state and reward from the environment. This feedback mechanism allows the filter to respond to noises dynamically.
- Low computational complexity: For $N = 10$, $S = 1000$, supDQN involves 1,024,573 computations as compared to a stack filter compared at the same efficiency, which involves 3,054,243 computations.
- Reduced delay: An n^{th} order filter introduces a delay of $n/2$, and stacking multiple (k) such filters results in a delay of $k \times n/2$. supDQN uses only one filter at any segment, producing the least delay.
- Minimized error and loss of information: The average normalized RMSE of supDQN is 1.1974, which is lesser than all other traditional filters. Additionally, thresholding in wavelet denoising may involve some loss of information, which is avoided by frequency-based FIR filters employed in supDQN.

The proposed filtering technique in this study still needs more confidence to achieve filtering in minimal time. However, efforts have been made in this study to reduce the time consumption of the process by replacing higher-order filters with lower-order filters. In the future, this work can be modified to achieve faster filtering and make it feasible

for prostheses. Additionally, the rewarding strategy could be improved, which can identify the contribution of different noises in a noise-overlapped environment. However, this study's outcomes can be used in applications requiring a clean sEMG signal without time constraints, such as extended analytical research on clean sEMG signal, rehabilitation, clinical study, medical condition diagnosis, etc. In the future, this study can be extended to achieve faster filtering or filtering at lower noise levels to integrate with prosthetic devices. Additionally, to avoid the impact of noise level on the filtering, more advanced features can be explored that may provide better differentiation between noisy and clean signals at lower noise levels. Deep learning architecture can be exploited to do the same.

ETHICS APPROVAL

This study was performed in accordance with the Declaration of Helsinki. This study on humans was approved by Malaviya National Institute of Technology Jaipur. All the adult participants provided their written informed consent to participate in this study.

REFERENCES

[1] Clarivate. (1997). *Statistical Data of sEMG Related Research: Web of Science*. [Online]. Available: https://www.webofscience.com/wos/woscc/summary/9fa9306b-c055-469b-914a-6cbb48ec0c49-b421cf41/relevance/1

[2] D. F. Stegeman, J. H. Blok, H. J. Hermens, and K. Roeleveld, "Surface EMG models: Properties and applications," *J. Electromyogr. Kinesiol.*, vol. 10, no. 5, pp. 313–326, Oct. 2000.

[3] G. Boccia, D. Dardanello, V. Rosso, L. Pizzigalli, and A. Rainoldi, "The application of sEMG in aging: A mini review," *Gerontology*, vol. 61, no. 5, pp. 477–484, 2015.

[4] C. Frigo and P. Crenna, "Multichannel SEMG in clinical gait analysis: A review and state-of-the-art," *Clin. Biomechanics*, vol. 24, no. 3, pp. 236–245, Mar. 2009.

[5] M. B. I. Reaz, M. S. Hussain, and F. Mohd-Yasin, "Techniques of EMG signal analysis: Detection, processing, classification and applications," *Biol. Procedures Online*, vol. 8, no. 1, pp. 11–35, Dec. 2006.

[6] C. J. De Luca, L. D. Gilmore, M. Kuznetsov, and S. H. Roy, "Filtering the surface EMG signal: Movement artifact and baseline noise contamination," *J. Biomechanics*, vol. 43, no. 8, pp. 1573–1579, May 2010.

[7] J. M. DeFreitas, T. W. Beck, and M. S. Stock, "Comparison of methods for removing electromagnetic noise from electromyographic signals," *Physiol. Meas.*, vol. 33, no. 2, pp. 147–158, Feb. 2012.

[8] C. J. De Luca, M. Kuznetsov, L. D. Gilmore, and S. H. Roy, "Inter-electrode spacing of surface EMG sensors: Reduction of crosstalk contamination during voluntary contractions," *J. Biomechanics*, vol. 45, no. 3, pp. 555–561, Feb. 2012.

[9] A. Phinyomark, C. Limsakul, and P. Phukpattaranont, "A comparative study of wavelet denoising for multifunction myoelectric control," in *Proc. Int. Conf. Comput. Autom. Eng.*, Mar. 2009, pp. 21–25.

[10] A. O. Andrade, S. Nasuto, P. Kyberd, C. M. Sweeney-Reed, and F. R. Van Kanijn, "EMG signal filtering based on empirical mode decomposition," *Biomed. Signal Process. Control*, vol. 1, no. 1, pp. 44–55, Jan. 2006.

[11] L. Liu, P. Liu, E. A. Clancy, E. Scheme, and K. B. Englehart, "Signal whitening preprocessing for improved classification accuracies in myoelectric control," in *Proc. IEEE 37th Annu. Northeast Bioeng. Conf. (NEBEC)*, Apr. 2011, pp. 1–2.

[12] C. Tapia, O. Daud, and J. Ruiz-del-Solar, "EMG signal filtering based on independent component analysis and empirical mode decomposition for estimation of motor activation patterns," *J. Med. Biol. Eng.*, vol. 37, no. 1, pp. 140–155, Feb. 2017.

[13] R. M. Howard, R. Conway, and A. J. Harrison, "An exploration of eliminating cross-talk in surface electromyography using independent component analysis," in *Proc. 26th Irish Signals Syst. Conf. (ISSC)*, Jun. 2015, pp. 1–6.

[14] P. Parker, K. Englehart, and B. Hudgins, "Myoelectric signal processing for control of powered limb prostheses," *J. Electromyogr. Kinesiol.*, vol. 16, no. 6, pp. 541–548, Dec. 2006.

[15] J. Wu, X. Li, W. Liu, and Z. Jane Wang, "SEMG signal processing methods: A review," *J. Phys., Conf. Ser.*, vol. 1237, no. 3, Jun. 2019, Art. no. 032008.

[16] B. Widrow and E. Walach, "Adaptive signal processing for adaptive control," *IFAC Proc. Volumes*, vol. 16, no. 9, pp. 7–12, 1983.

[17] T. S. Alexander, *Adaptive Signal Processing: Theory and Applications*. New York, NY, USA: Springer, 2012.

[18] B. Widrow, J. R. Glover, J. M. McCool, J. Kaunitz, C. S. Williams, R. H. Hearn, J. R. Zeidler, J. E. Dong, and R. C. Goodlin, "Adaptive noise cancelling: Principles and applications," *Proc. IEEE*, vol. 63, no. 12, pp. 1692–1716, Dec. 1975.

[19] N. Iqbal, "DeepSeg: Deep segmental denoising neural network for seismic data," *IEEE Trans. Neural Netw. Learn. Syst.*, vol. 34, no. 7, pp. 3397–3404, Sep. 2023.

[20] K.-C. Wang, K.-C. Liu, S.-Y. Peng, and Y. Tsao, "ECG artifact removal from single-channel surface EMG using fully convolutional networks," in *Proc. IEEE Int. Conf. Acoust., Speech Signal Process. (ICASSP)*, Jun. 2023, pp. 1–5.

[21] A. Jena, P. Sharma, N. Gehlot, A. Vijayvargiya, and R. Kumar, "Efficient contaminant identification in sEMG signals using machine learning," in *Proc. 3rd Int. Conf. Power, Control Comput. Technol. (ICPC2T)*, Jan. 2024, pp. 25–30.

[22] J. Kober, J. A. Bagnell, and J. Peters, "Reinforcement learning in robotics: A survey," *Int. J. Robot. Res.*, vol. 32, no. 11, pp. 1238–1274, Sep. 2013.

[23] V. Mnih, K. Kavukcuoglu, D. Silver, A. Graves, I. Antonoglou, D. Wierstra, and M. Riedmiller, "Playing Atari with deep reinforcement learning," 2013, *arXiv:1312.5602*.

[24] F. Sahba and H. R. Tizhoosh, "Filter fusion for image enhancement using reinforcement learning," in *Proc. Can. Conf. Electr. Comput. Eng. Toward Caring Humane Technol. (CCECE)*, May 2003, pp. 847–850.

[25] R. Furuta, N. Inoue, and T. Yamasaki, "PixelRL: Fully convolutional network with reinforcement learning for image processing," *IEEE Trans. Multimedia*, vol. 22, no. 7, pp. 1704–1719, Jul. 2020.

[26] M. Alolaiwy, M. Tanik, and L. Jololian, "From CNNs to adaptive filter design for digital image denoising using reinforcement Q-learning," in *Proc. SoutheastCon*, Mar. 2021, pp. 1–8.

[27] C. Liang, H. Lin, and H. Ma, "Reinforcement learning-based denoising model for seismic random noise attenuation," *IEEE Trans. Geosci. Remote Sens.*, vol. 61, 2023, Art. no. 5908217.

[28] Á. L. V. Caraguay, J. P. Vásconez, L. I. B. López, and M. E. Benalcázar, "Recognition of hand gestures based on EMG signals with deep and double-deep Q-networks," *Sensors*, vol. 23, no. 8, p. 3905, Apr. 2023.

[29] M. C. Tosin and A. Balbinot, "Identification and removal of contaminants in sEMG recordings through a methodology based on fuzzy inference and actor-critic reinforcement learning," *Expert Syst. Appl.*, vol. 206, Nov. 2022, Art. no. 117772.

[30] *Data Acquisition, Loggers, Amplifiers, Transducers, Electrodes: Biopac*. Accessed: Feb. 22, 2023. [Online]. Available: https://www.biopac.com/

[31] A. Vijayvargiya, V. Gupta, R. Kumar, N. Dey, and J. M. R. S. Tavares, "A hybrid WD-EEMD sEMG feature extraction technique for lower limb activity recognition," *IEEE Sensors J.*, vol. 21, no. 18, pp. 20431–20439, Sep. 2021.

[32] C. Sinderby, L. Lindstrom, and A. E. Grassino, "Automatic assessment of electromyogram quality," *J. Appl. Physiol.*, vol. 79, no. 5, pp. 1803–1815, Nov. 1995.

[33] M. Boyer, L. Bouyer, J.-S. Roy, and A. Campeau-Lecours, "Reducing noise, artifacts and interference in single-channel EMG signals: A review," *Sensors*, vol. 23, no. 6, p. 2927, Mar. 2023.

[34] G. D. Fraser, A. D. C. Chan, J. R. Green, and D. T. MacIsaac, "Automated biosignal quality analysis for electromyography using a one-class support vector machine," *IEEE Trans. Instrum. Meas.*, vol. 63, no. 12, pp. 2919–2930, Dec. 2014.

[35] F. Duan, X. Ren, and Y. Yang, "A gesture recognition system based on time domain features and linear discriminant analysis," *IEEE Trans. Cogn. Develop. Syst.*, vol. 13, no. 1, pp. 200–208, Mar. 2021.

[36] G. P. Zhang, "Neural networks for classification: A survey," *IEEE Trans. Syst., Man, Cybern. C, Appl. Rev.*, vol. 30, no. 4, pp. 451–462, Nov. 2000.
[37] M. T. Ribeiro, S. Singh, and C. Guestrin, "'Why should I trust you' Explaining the predictions of any classifier," in *Proc. 22nd ACM SIGKDD Int. Conf. Knowl. Discovery Data Mining*, Aug. 2016, pp. 1135–1144.
[38] A. Vijayvargiya, P. Singh, R. Kumar, and N. Dey, "Hardware implementation for lower limb surface EMG measurement and analysis using explainable AI for activity recognition," *IEEE Trans. Instrum. Meas.*, vol. 71, pp. 1–9, 2022.
[39] A. Vijayvargiya, A. Raghav, A. Bhardwaj, N. Gehlot, and R. Kumar, "A LIME-based explainable machine learning technique for the risk prediction of chronic kidney disease," in *Proc. Int. Conf. Comput., Electron. Electr. Eng. Appl. (IC2E3)*, Jun. 2023, pp. 1–6.
[40] Y. Kopsinis and S. McLaughlin, "Development of EMD-based denoising methods inspired by wavelet thresholding," *IEEE Trans. Signal Process.*, vol. 57, no. 4, pp. 1351–1362, Apr. 2009.

ASHUTOSH JENA received the B.Tech. degree in electrical engineering from Veer Surendra Sai University of Technology, Burla, Odisha, India, in 2021. Currently, he is pursuing the Ph.D. degree with the Malaviya National Institute of Technology Jaipur, Rajasthan, India. His research interests include biomedical signal processing, machine learning, and reinforcement learning.

NAVEEN GEHLOT (Graduate Student Member, IEEE) received the B.Tech. degree (Hons.) in electrical and electronics engineering from Rajasthan Technical University, Kota, India, in 2016, and the M.E. degree (Hons.) in control system from M.B.M. Engineering College, Jodhpur, India, in 2021. He is currently pursuing the Ph.D. degree with the Department of Electrical Engineering, MNIT Jaipur, India. His research interests include biomedical signal processing, intelligent control techniques, and robotic hand control.

RAJESH KUMAR (Senior Member, IEEE) received the B.Tech. degree (Hons.) in electrical engineering from the National Institute of Technology (NIT), Kurukshetra, India, in 1994, and the M.E. (Hons.) and Ph.D. degrees in power systems and intelligent systems from the Malaviya National Institute of Technology (MNIT) Jaipur, Rajasthan, India, in 1997 and 2005, respectively. He was a Postdoctoral Research Fellow with the Department of Electrical and Computer Engineering, National University of Singapore (NUS), Singapore, from 2009 to 2011. Since 1995, he has been a Faculty Member with the Department of Electrical Engineering, MNIT Jaipur, where he is currently working as a Professor. His research interests include intelligent systems, data-driven algorithms and analytics, smart grids, biomedical (signal processing and image processing), and optimization. He has been an Associate Editor of IEEE Access, IEEE Industrial Electronics Technology News (ITeN), *Swarm and Evolutionary Computation* (Elsevier), IET Renewable and Power Generation, IET Power Electronics, International Journal of Bio-Inspired Computing, and *CAAI Transactions on Intelligence Technology - IET*. He is appointed as a Distinguished Lecturer with IEEE IAS, in 2024 and 2025.

ANKIT VIJAYVARGIYA (Senior Member, IEEE) received the B.Tech. degree (Hons.) in electrical engineering from Rajasthan Technical University, Kota, India, in 2010, the M.Tech. degree in instrumentation from Devi Ahilya University, Indore, India, in 2014, and the Ph.D. degree in electrical engineering from the Malaviya National Institute of Technology Jaipur, India. Currently, he is a Postdoctoral Researcher with Dublin City University. He is also an Associate Professor with the Department of Electrical Engineering, Swami Keshvanand Institute of Technology, Management and Gramothan, Jaipur. His research interests include biomedical signal processing, pattern recognition, and machine learning.

MAHIPAL BUKYA (Senior Member, IEEE) received the B.Tech. degree in electrical and electronics engineering from the BVRIT, JNTU Hyderabad, India, the M.E. degree in electrical engineering from Indian Institute of Science (IISc), Bengaluru, India. Currently, he is pursuing the Ph.D. degree with the Malaviya National Institute of Technology (MNIT) Jaipur, Rajasthan, India. He has been a Faculty Member with the Department of Electrical and Electronics Engineering, Manipal Academy of Higher Education, MIT-Bengaluru, where he is an Assistant Professor (Senior-Scale). His research interests include electrical vehicle (EV), EV cabling networks, EV protection, electromagnetic fields, high voltage engineering, and AI ML applications in EVs.